Research Square

Preprints are preliminary reports that have not undergone peer review.
They should not be considered conclusive, used to inform clinical practice,
or referenced by the media as validated information.

Host-Directed p53 and NRF2 Co-Activation Reverses Acute COVID-19 and Long COVID Pathology by Restoring the miR-29 and miR-145 Epigenetic Axis

Boominathan Lakshmanane

drboomi@genomediscovery.org

genomediscovery.org https://orcid.org/0009-0008-5358-7462

Research Article

Keywords: Host-directed therapy (HDT) p53 and NRF2 co-activation SARS-CoV-2 / COVID-19 Long COVID (Post-Acute Sequelae of SARS-CoV-2, PASC) Epigenetic axis restoration miR-29 family (11-site viral targeting) miR-145 epigenetic shielding

Posted Date: November 19th, 2026

DOI: https://doi.org/10.21203/rs.3.rs-11779577/v1

License: This work is licensed under a Creative Commons Attribution 4.0 International License.
Read Full License

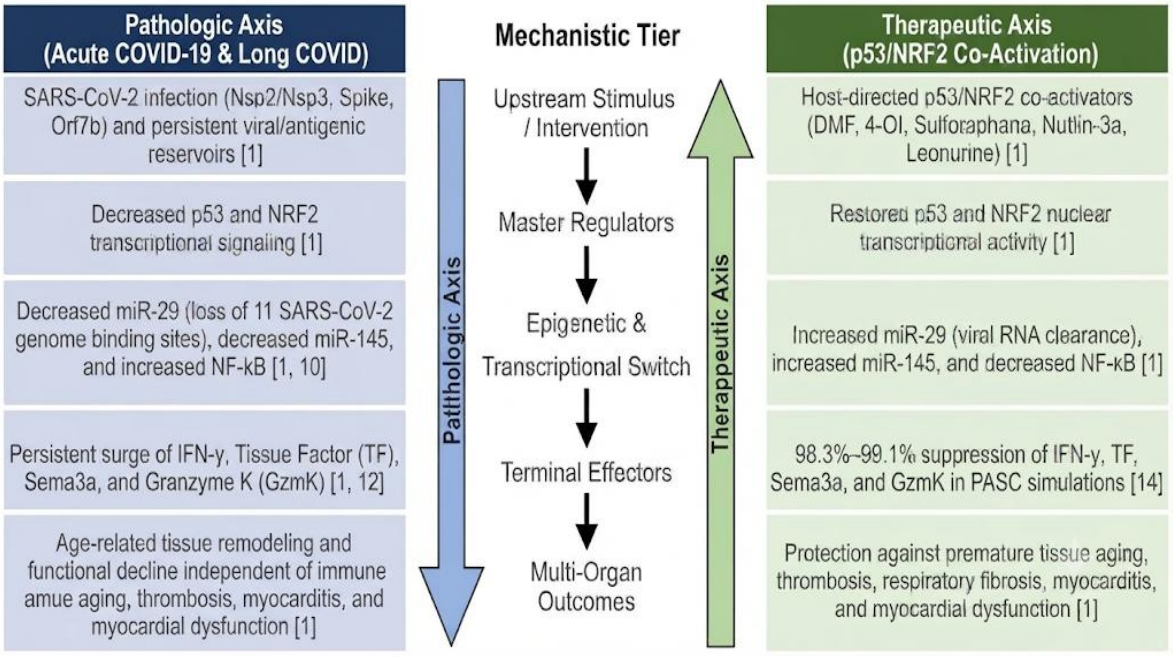
Additional Declarations: The authors declare no competing interests.

Host-Directed p53 and NRF2 Co-Activation Reverses Acute COVID-19 and Long COVID Pathology by Restoring the miR-29 and miR-145 Epigenetic Axis

Dr. L. Boominathan, PhD
Founder and Director-President, Genome-2-BioMedicine Discovery Center (GBMD), Puducherry-4, India
Web: www.genomediscovery.org | Email: Drboomi@genomediscovery.org; genomdiscovery@gmail.com | Phone: +91-413-2960879

Graphical Abstract

Graphical abstract. Unified Pathologic and Therapeutic Signaling Architecture of p53 and NRF2 in **COVID-19 and Long COVID.**



Abstract

Despite over 524,592 COVID-19 papers indexed in PubMed as documented in our synthesis compilation and widespread vaccine deployment over the past six years, COVID-19 has caused more than 7.11 million officially reported deaths globally—with WHO excess mortality estimates reaching 14.83 million for 2020–2021 alone and cumulative excess death estimates spanning 18.5 to 35.2 million [1, 2, 3, 4, 5, 6]—while leaving an estimated 400 million individuals worldwide with Long COVID (post-acute sequelae of SARS-CoV-2, or PASC) at an approximate $1 trillion annual economic cost [1, 5]. To address the absence of a phase-independent mechanistic therapy, we propose and computationally evaluate a unified host-directed therapeutic framework centered on co-activating the cellular stress-response regulators p53 and NRF2 [1]. Across acute and post-acute phases, SARS-CoV-2 suppresses p53 and NRF2 signaling, depleting miR-29 (which harbors 11 conserved binding sites on the SARS-CoV-2 genome and directly targets IFNG) and miR-145 (which restrains Tissue Factor F3, Semaphorin-3A Sema3a, Granzyme K GZMK, and MYC) while hyperactivating NF-κB [1, 7, 8, 9, 10]. This upstream collapse drives persistent elevations in IFN-γ, Tissue Factor (TF), Sema3a, and Granzyme K (GzmK), promoting myocarditis, thromboembolism, myocardial dysfunction, and age-related tissue remodeling independently of age-associated immune dysfunction [1, 11, 12, 13].

Stiff ordinary differential equation (ODE) simulations (solve_ivp/BDF) parameterized from published turnover kinetics demonstrate that simulated p53/NRF2 co-activation induces a sharp bifurcation switch near an agonist threshold of Uth = 0.4–0.6 under persistent antigenic stimulation, producing a 13.75-fold recovery of miR-29 and a 54.39-fold recovery of miR-145 while suppressing NF-κB by 94.0% and reducing IFN-γ, TF, Sema3a, and GzmK by 98.3% to 99.1% in locked PASC steady states [14]. In an aggressive acute infection simulation (rv = 0.12 h-1), therapy initiated at 24 h lowers 168 h viral load by 46.2% and suppresses the four terminal effectors by 92.0% to 95.1% [14]. Because these quantitative dynamics derive from in silico modeling and cross-study synthesis, key evidentiary caveats remain—including incomplete extraction of individual duplex coordinates for all 11 miR-29 viral sites, cross-species differences in miR-145 validation for GZMK and Sema3a, compartment-specific p53 paradoxes, and the absence of prospective randomized trials testing combined p53/NRF2 agonism in PASC [1, 10, 15].

The Mechanistic Impasse Across Acute COVID-19 and Long COVID

By late 2026, WHO sentinel surveillance confirms continued global SARS-CoV-2 circulation across Omicron descendant lineages such as JN.1, NB.1.8.1, XFG, and PQ.16.1.1, while cumulative Long COVID cases represent a visible floor of roughly 400 million people worldwide, with stress-adjusted burden models

warning of higher cumulative prevalence under repeated reinfections [2, 16, 17]. Clinical cohorts indicate that nearly 70% of Long COVID patients experience dysautonomia and roughly 58% develop myalgic encephalomyelitis/chronic fatigue syndrome (ME/CFS) characterized by post-exertional malaise, yet no FDA-approved disease-modifying treatment exists [1, 18]. Direct-acting antivirals and vaccines mitigate acute mortality, but they do not reverse persistent host transcriptional hijacking, microvascular endotheliitis, cardiac neurovascular disruption, or progressive organ decline once viral structural or accessory proteins reprogram host stress checkpoints [1, 19, 20, 21].

A major obstacle to curative drug design has been treating COVID-19 coagulopathy, myocarditis, pulmonary fibrosis, neurocognitive decline, and accelerated organ aging as disconnected complications [1, 4, 22]. Synthesizing 21 core peer-reviewed studies with multi-scale systems analyses from the Genome-2-BioMedicine Discovery Center (GBMD) establishes that these manifestations converge on a single bidirectional switch [1]. In the pathologic axis, COVID-19 infection decreases host p53 and NRF2 activity, suppressing miR-29 and miR-145 while increasing NF-κB; this drives surges in IFN-γ, TF, Sema3a, and GzmK that precipitate myocarditis, myocardial dysfunction, thrombosis, and immune-independent tissue remodeling [1]. In the therapeutic axis, p53/NRF2-based therapy restores p53 and NRF2 signaling, re-inducing miR-29 (enabling 11-site viral genome targeting) and miR-145 while suppressing NF-κB, thereby downregulating IFN-γ, TF, Sema3a, and GzmK across both acute and chronic phases [1].

Results

SARS-CoV-2 Suppresses Host p53 and NRF2 Checkpoints Across Phases

Converging molecular and clinical evidence demonstrates that SARS-CoV-2 directly impairs both NRF2 and p53 host defense networks [1]. Olagnier et al. showed that NRF2-driven antioxidant and anti-inflammatory gene expression is suppressed in lung biopsies from COVID-19 patients and in SARS-CoV-2-infected airway cells, whereas pharmacological reactivation with the NRF2 agonists 4-octyl-itaconate (4-OI) and dimethyl fumarate (DMF) elicits a potent antiviral and anti-inflammatory program that restricts viral replication [1, 9, 23]. Concurrently, Gómez-Carballa et al. reported that SARS-CoV-2 Nsp2 and Nsp3 proteins hijack and promote p53 degradation, and that TP53 transcript levels are significantly downregulated in the blood of severe COVID-19 patients—a deficit persisting for at least 24 weeks post-infection in Long COVID cohorts [1, 19]. Extending these findings, Zhang and El-Deiry demonstrated that transfected SARS-CoV-2 spike expression in mammalian cells inhibits p53-mediated activation of p21(WAF1), TRAIL death receptor DR5, and MDM2, confirming multi-protein viral interference with p53 transcriptional fidelity [1, 8].

Complementary systems modeling across GBMD preprints demonstrates how this upstream checkpoint loss propagates across accessory non-coding and metabolic circuits [1, 20]. SARS-CoV-2 accessory protein Orf7b induces the master oncogene MYC (c-Myc), which hypertranscribes linear, circular, and extrachromosomal DNA isoforms of the long non-coding RNA PVT1 to sponge protective host microRNAs including miR-24-3p, miR-145-5p, miR-214, and miR-519d-3p [1, 20]. Depletion of miR-24-3p derepresses KEAP1 to accelerate proteasomal NRF2 turnover, while PVT1-mediated microRNA sequestration unleashes HIF-1α/HIF-2α, transferrin receptor 1 (TFRC), and CCL2-driven microvascular endotheliitis [1,

20, 21, 24]. Simultaneously, viral induction of REST and IL-6/STAT3 elevates circulating miR-21-5p in hospitalized COVID-19 patients under 55 years of age—where high miR-21-5p predicts critical disease (OR = 4.19), invasive mechanical ventilation (OR = 5.63), and mortality (OR = 6.00)—directly targeting TP53 (ΔG = -21.8 kcal/mol), PTEN (ΔG = -24.6 kcal/mol), and STK11 (LKB1; ΔG = -22.4 kcal/mol) to blunt AMPK energy sensing and somatic stem-cell self-renewal [1, 25]. Loss of nuclear p53 and NRF2 further disables SIRT3 and TFAM transcription, halting LC3-mediated nucleoid-phagy and leaving leaked cytosolic mitochondrial DNA to sustain cGAS-STING and NLRP3 inflammasome activation [1, 26].

Epigenetic Collapse of miR-29 and miR-145 Derepresses Viral Replication and NF-κB Signaling

Downregulation of p53 and NRF2 removes the transcriptional drivers required to sustain miR-29 and miR-145 [1]. On the miR-29 arm, Xi et al. showed that the p53/miR-29a-3p axis mediates the antifibrotic effects of leonurine in angiotensin II-stimulated cardiac fibroblasts, while Tian et al. demonstrated that restoring NRF2 attenuates myocardial ischemia-reperfusion injury via the miR-29a-3p/CCNT2 axis [1]. Kurinna et al. further established a direct Nrf2–miR-29–desmocollin-2 axis governing epithelial desmosome integrity, and Xiao et al. used single-cell RNA sequencing to confirm that NRF2 regulates vascular smooth muscle cell phenotypic switching and structural integrity [1]. On the miR-145 arm, Sachdeva et al. established that p53 directly binds a p53 response element in the MIR145 promoter to induce miR-145, which in turn post-transcriptionally represses MYC [1]. Because c-Myc and Bach1 also increase with age to repress MIR145 and inhibit NRF2 adaptive homeostasis, loss of p53/NRF2 creates a self-reinforcing epigenetic trap [1, 22].

Clinical studies verify that both microRNAs are depleted during SARS-CoV-2 infection [1]. Kim et al. observed significant dysregulation of circulating miR-29a-3p alongside elevated thrombospondin-1 in severe COVID-19 [1, 27], while Gambardella et al. showed that exosomal miR-145 and miR-885 are markedly reduced in COVID-19 patients, correlating inversely with D-dimer and promoting endothelial apoptosis, impaired angiogenesis, and thrombosis [1, 28]. Crucially, miR-29 loss also dismantles direct host sequence-level antiviral restriction: Jafarinejad-Farsangi et al. performed genome-wide in silico binding analysis and identified the miR-29 family (miR-29a, miR-29b, and miR-29c) as possessing the highest number of binding sites on the SARS-CoV-2 genome—11 binding sites total (Figure 2), including 5 sites for hsa-miR-29a-3p and 4 sites for hsa-miR-29c-3p—clustered across ORF1ab, Spike (S), and Nucleocapsid (N) coding regions [1, 10, 29]. These interactions satisfied strict seed complementarity, alignment scores ≥ 150, and thermodynamic thresholds (ΔG > -20 kcal/mol, with none below -29 kcal/mol), while displaying 100% sequence conservation across SARS-CoV-2 isolates from 10 countries (United States, Spain, France, Japan, South Africa, India, Brazil, Australia, South Korea, and Kazakhstan) [10].

Downstream Effector Convergence: IFN-γ, Tissue Factor, Semaphorin-3A, and Granzyme K

With p53/NRF2 suppressed, miR-29 and miR-145 depleted, and NF-κB activated, four terminal effectors drive multi-organ COVID-19 and Long COVID pathology [1]. First, IFN-γ—which is directly targeted by miR-

29 to restrain innate and adaptive immunity as established by Ma et al. [1]—is persistently elevated across acute and chronic phases. Krishna et al. documented spontaneous, persistent, T cell-dependent IFN-γ release in patients progressing to Long COVID, observing that symptom recovery tracked the normalization of IFN-γ to baseline [1, 12, 30]. Li et al. used comparative single-cell RNA-seq to implicate IFN-γ as a causal driver of post-acute respiratory sequelae, demonstrating that post-infection IFN-γ neutralization attenuates lung inflammation and fibrosis in mice [1, 31, 32], while Cao et al. showed that inhibiting CXCL10 and IFN-γ ameliorates myocarditis in preclinical models of SARS-CoV-2 mRNA vaccination [1, 13, 33].

Second, Tissue Factor (TF / F3) is derepressed by exosomal miR-145 loss and unrestrained NF-κB signaling [1, 28]. Sahu et al. demonstrated that miR-145 impedes venous thrombus formation by directly targeting F3, and that restoring miR-145 reduces TF activity and thrombogenesis [1, 7]. In severe COVID-19 and PASC, TF upregulation is compounded by inflammasome/GSDMD-mediated pyroptosis and NINJ1-dependent plasma membrane rupture, which releases pro-coagulant TF-positive microvesicles [34, 35, 36], as well as by Long COVID extracellular vesicle (LC-EV) induction of RUNX2, MYC-driven lncRNA MEG3, and SIRT6 loss [22]. Third, Semaphorin-3A (Sema3a) links miR-145 depletion directly to cardiac neurovascular dysfunction: Wagner et al. (Science, 2023) established that aging downregulates endothelial miR-145, and that miR-145 deletion increases Sema3a expression, reducing ventricular axon density, altering heart rate patterns, and increasing electrical instability [1, 11, 37]. Extrapolated to COVID-19 patients—who exhibit pronounced reductions in p53/NRF2 and circulating miR-145 [1, 28]—Sema3a derepression offers a coherent mechanism for post-COVID arrhythmias, autonomic dysfunction, and myocardial injury alongside CCL2-mediated endothelial-cardiomyocyte uncoupling [1, 21].

Fourth, Granzyme K (GzmK) bridges chronic inflammation to premature organ aging [1]. Jonsson et al. showed that GzmK+ CD8+ T cells (TteK cells) form a core cytokine-producing population enriched across inflamed human tissues, including COVID-19 bronchoalveolar lavage fluid [1]. Allen et al. (Immunity, 2026) demonstrated that NF-κB-activated fibroblasts orchestrate inflammaging and the emergence of pro-inflammatory GzmK+ T cells [1, 38], and Kannangara et al. (Immunity, 2026) showed in young and aged Gzmk−/− mice that Granzyme K drives age-related tissue remodeling and functional decline—including renal complement deposition and hepatic TGF-β-associated fibrosis—independently of age-associated immune dysfunction [1]. Crucially, Qi et al. demonstrated in a murine myocardial ischemia-reperfusion model that sevoflurane postconditioning protects against cardiac injury by upregulating miR-145 and downregulating GZMK expression [1, 39], linking p53/NRF2–miR-145 restoration directly to GzmK suppression [1] (Figure 2).

Non-Linear Stiff ODE Kinetic Modeling and Bifurcation Reversal

To test phase-independent reversibility quantitatively, we constructed a nine-variable stiff ODE network coupling SARS-CoV-2 viral load (V), p53/NRF2 axis activity (P), miR-29 (M_29), miR-145 (M_145), NF-κB (N), IFN-γ (I_γ), TF, Sema3a (S_3), and GzmK (GK), solved via Python scipy.integrate.solve_ivp using the Backward Differentiation Formula (BDF) [14] (Figure 3).

Biological State / Simulation Scenario	Viral Load (V)	p53/NRF2 (P)	miR-29 (M_29)	miR-145 (M_145)	NF-κB (N)	IFN-γ (I_γ)	TF	Sema3a (S_3)	GzmK (GK)
Healthy Baseline Steady State (S_ext = 0, U_th = 0)	0.0000	1.0000	3.3697	3.7885	0.0571	0.0896	0.1112	0.2088	0.1303
Aggressive Acute Untreated at 168 h (r_v = 0.12 h^{-1})	4.355	0.152	0.233	0.068	5.327	11.412	11.412	14.043	17.233
Aggressive Acute Treated at 24 h (U_th = 1.1; 168 h)	2.344	1.032	1.721	1.346	1.301	0.560	0.689	1.125	0.897
PASC Locked Steady State (S_ext = 0.05, U_th = 0)	4.5700	0.1421	0.2128	0.0602	5.8102	12.6301	12.4661	15.2499	18.8474
PASC Rescued at 504 h (U_th = 1.1 started at 72 h)	0.7856	1.9084	2.9254	3.2749	0.3482	0.1335	0.1398	0.2579	0.1680

In the chronic Long COVID simulation sustained by a persistent antigenic/viral reservoir (S_ext = 0.05), the untreated steady state locks into severe dysregulation: p53/NRF2 falls by 85.8% (1.0000 to 0.1421), miR-29 falls by 93.7% (3.3697 to 0.2128), and miR-145 falls by 98.4% (3.7885 to 0.0602), driving a 101.8-fold rise in NF-κB (5.8102), a 141.0-fold rise in IFN-γ (12.6301), a 112.1-fold rise in TF (12.4661), a 73.0-fold rise in Sema3a (15.2499), and a 144.6-fold rise in GzmK (18.8474) [14]. Introducing p53/NRF2 co-activation therapy (U_th = 1.1) at t = 72 h reverses this pathological basin by day 21 (t = 504 h): p53/NRF2 recovers 13.43-fold (1.9084), miR-29 recovers 13.75-fold (2.9254), miR-145 recovers 54.39-fold (3.2749), persistent viral load falls by 82.8% (4.5700 to 0.7856), NF-κB drops by 94.0%, IFN-γ drops by 98.9%, TF drops by 98.9%, Sema3a drops by 98.3%, and GzmK drops by 99.1% [14]. Similarly, in the aggressive acute infection scenario (r_v = 0.12 h^{-1}, V_0 = 1.5), initiating therapy at 24 h reduces 168 h viral load by 46.2% (4.355 to 2.344) and cuts IFN-γ, TF, Sema3a, and GzmK by 95.1%, 94.0%, 92.0%, and 94.8%, respectively [14] (Figure 4).

Pharmacological Repositioning, Pan-Viral Generalizability, and Safety Trade-Offs

Several approved and investigational agents can be repositioned to co-activate this axis [1, 22, 25] (Figure 5). In the NRF2 arm, clinically approved dimethyl fumarate (DMF) and 4-octyl-itaconate (4-OI) alkylate KEAP1 to drive nuclear NRF2 translocation and suppress SARS-CoV-2 replication and inflammatory signaling [1, 9, 23]. Sulforaphane disrupts KEAP1 to activate NRF2/ARE-driven PARK2 (Parkin) and miR-

29/145 networks [1, 22, 25], leonurine stimulates the p53/miR-29a-3p antifibrotic pathway in cardiac fibroblasts [1], and sevoflurane elevates miR-145 to downregulate GZMK in myocardial ischemia-reperfusion [1, 39]. On the p53 and metabolic side, Nutlin-3a and MDM2 antagonists stabilize p53 to transactivate MIR145 and MIR29 [1, 25], while metformin inhibits c-Myc, activates AMPK/SIRT6, attenuates Spike-induced α-synuclein aggregation, and showed a 0.7 percentage-point lower risk of clinician-diagnosed Long COVID versus placebo in a quadruple-blinded randomized trial (95% CrI -1.5 to 0.1; posterior probability of efficacy 0.96) [22, 40, 41]. Adjunctive 25-hydroxyvitamin D and sitagliptin activate SIRT6 to suppress RUNX2, NF-κB, TF, and PCSK9-mediated vascular remodeling [1, 22]. Furthermore, because RSV promotes p53 degradation and NRF2 loss [1], and Influenza A virus, EBV, HBV, HCV, HIV-1, and HPV conservedly elevate c-Myc and disrupt p53/miR-145 checkpoints [26], p53/NRF2 co-activation represents a candidate mutation-resistant, host-directed preparedness strategy [1] (Figure 6).

Translation nonetheless demands disciplined management of three biological trade-offs. First, p53 can transcriptionally repress HNF4A, which drives macrophage peroxisome biogenesis required for alveolar repair and QPRT-dependent de novo NAD+ biosynthesis protecting against acute kidney injury [15]; co-administering SIRT1/SIRT6 activators or NAD+ precursors (nicotinamide or nicotinamide riboside) alongside low-dose p53/NRF2 agonists is therefore advisable to preserve epithelial regeneration [15]. Second, genotoxic p53 inducers (such as doxorubicin or cisplatin) risk exacerbating acute alveolar apoptosis during ARDS, favoring non-genotoxic MDM2 antagonists or natural/clinical NRF2-SIRT6 modulators titrated to the U_th = 0.6–1.1 therapeutic window [14, 25]. Third, because constitutive somatic NRF2 hyperactivation can confer cytoprotection to occult tumors [1], chronic Long COVID regimens should employ pulsatile or biomarker-guided dosing rather than continuous high-dose exposure.

Discussion and Mechanistic Caveats

Integrating the p53/NRF2–miR-29/145–NF-κB switch provides a unified mechanistic explanation for why an acute respiratory virus produces persistent cardiovascular, thrombotic, pulmonary, and premature-aging sequelae months or years after initial infection [1, 3, 19]. Rather than attributing Long COVID to unconnected organ pathologies, our model links viral genome persistence, T cell-dependent IFN-γ secretion, exosomal miR-145-loss thrombosis, Sema3a-mediated cardiac denervation, and fibroblast–GzmK+ T-cell tissue remodeling to a single reversible regulatory node [1, 11, 12, 28, 38].

Four evidentiary limitations warrant explicit acknowledgment prior to clinical translation. First, while Jafarinejad-Farsangi et al. documented 11 conserved miR-29 binding sites across the SARS-CoV-2 genome (5 in hsa-miR-29a-3p and 4 in hsa-miR-29c-3p) [10], exact nucleotide coordinates and individual duplex ΔG values from their supplementary table were not available in the extracted source text and require direct experimental Ago2-CLIP confirmation in infected human respiratory epithelium. Second, miR-145 repression of GZMK and derepression of Sema3a were demonstrated in murine myocardial ischemia-reperfusion and murine cardiac aging models, respectively [1, 11, 39]; cross-species 3'-UTR binding and functional silencing must be verified in human CD8+ TteK cells, NF-κB-activated lung fibroblasts, and human cardiac endothelial cells. Third, p53 exhibits tissue- and phase-dependent duality: while circulating leukocytes and spike-transfected cells show TP53 suppression [1, 8], Long COVID extracellular vesicles

can activate stress-responsive p53/p21 alongside RUNX2 in vascular cells [22], underscoring that therapeutic co-activation must restore balanced physiological checkpoint signaling rather than provoke maladaptive senescence or HNF4A repression [15, 22]. Fourth, because our kinetic trajectories derive from deterministic ODE simulations rather than longitudinal patient drug cohorts, prospective randomized trials stratifying participants by circulating miR-29a-3p, exosomal miR-145, IFN-γ, D-dimer, and GzmK are essential to validate the predicted bifurcation dose threshold in humans [1, 12, 27, 28].

Methods

Stiff Ordinary Differential Equation Formulation and Numerical Integration

The dynamic competition between SARS-CoV-2 hijacking and p53/NRF2 restoration was modeled via a nine-variable non-linear ODE system tracking viral load (V), p53/NRF2 axis (P), miR-29 (M_29), miR-145 (M_145), NF-κB (N), IFN-γ (I_γ), TF, Sema3a (S_3), and GzmK (GK) [14]:

dV/dt = r_v V (1 - V/K_v) - (d_v + k_m29_v M_29) V + S_ext
dP/dt = k_p_synth + U_th(t) - (d_p + k_p_viral V_eff) P
dM_29/dt = k_29_basal + k_29_p [P^2 / (K_p29^2 + P^2)] - (d_29 + k_29_v_sponge V_eff) M_29
dM_145/dt = k_145_basal + k_145_p [P^2 / (K_p145^2 + P^2)] - (d_145 + k_145_nfkb N) M_145
dN/dt = k_n_basal + k_n_viral V_eff - (d_n + k_n_p P) N
dI_γ/dt = k_ig_basal + [k_ig_n N / (1 + (M_29/K_29_ig)^2)] - d_ig I_γ
dTF/dt = k_tf_basal + [k_tf_n N / (1 + (M_145/K_145_tf)^2)] - d_tf TF
dS_3/dt = k_s3_basal + [k_s3_n (0.4 + N) / (1 + (M_145/K_145_s3)^2)] - d_s3 S_3
dGK/dt = k_gk_basal + [k_gk_n N / (1 + (M_145/K_145_gk)^2)] - d_gk GK

Bioinformatic and Regulatory Motif Pipeline

Single-cell RNA-seq processing for post-acute COVID-19 biopsies is structured in Seurat v5.0 using Wilcoxon rank-sum differential testing with Benjamini-Hochberg false discovery rate correction ($q < 0.05$) [1, 22]. Promoter and 3'-UTR regulatory motif verification uses JASPAR 2024/2026 position frequency matrices, ENCODE ChIP-seq tracks, and RNA duplex thermodynamics computed via ViennaRNA (v2.6.0) and RNAhybrid (v2.2) at 37°C [1, 22, 25].

Tables

Table 1: Pathologic Dysregulation in COVID-19 and Reversal by the p53/NRF2 Therapeutic Axis

Molecular Node / Effector	COVID-19 / PASC Pathologic State	Primary Pathophysiological Consequence	Reversal Mechanism Under p53/NRF2 Therapy	Key Supporting References
p53 / NRF2	Downregulated / degraded by Nsp2, Nsp3, Spike, and KEAP1/Orf7b	Loss of redox homeostasis, checkpoint fidelity, and miR-29/145 transcription	Co-activation restores nuclear p53/NRF2 transcriptional output and antioxidant defense	Olagnier et al. 2020; Gómez-Carballa et al. 2022; Zhang & El-Deiry 2024 [1]
miR-29 family (11 viral sites)	Suppressed in severe COVID-19; sponged by viral RNA	Loss of 11-site viral genome interference; elevated	Induced by p53/NRF2 to target SARS-CoV-2 RNA and repress IFNG	Jafarinejad-Farsangi et al. 2020; Kim et al. 2022; Ma et al. 2011; Xi et al.

		thrombospondin-1 and IFN-γ		2023; Tian et al. 2021 [1]
miR-145	Downregulated in circulation, exosomes, and aging endothelium	Unchecked MYC, F3 (TF), Sema3a, and GZMK; thrombosis and denervation	Transactivated by p53/NRF2; represses F3, Sema3a, GZMK, and MYC	Gambardella et al. 2023; Sachdeva et al. 2009; Sahu et al. 2017; Wagner et al. 2023; Qi et al. 2019 [1]
NF-κB	Hyperactivated in fibroblasts, endothelium, and immune cells	Sustained cytokine transcription, fibroblast inflammaging, emergence of GzmK+ T cells	Antagonized by NRF2/p53 and SIRT6, halting stromal-immune amplification	Allen et al. 2026; Olagnier et al. 2020 [1, 22]
IFN-γ	Spontaneously and persistently elevated across acute and Long COVID	Respiratory fibrosis/sequelae and post-infection/mRNA-vaccine myocarditis	Direct post-transcriptional repression by restored miR-29 and NF-κB attenuation	Krishna et al. 2024; Li et al. 2024; Cao et al. 2025; Ma et al. 2011 [1]
Tissue Factor (TF / F3)	Upregulated via miR-145 loss and pyroptotic microvesicles	Venous/arterial thrombosis, elevated D-dimer, and microvascular occlusion	Directly silenced by restored miR-145 and endothelial SIRT6/NF-κB restraint	Sahu et al. 2017; Gambardella et al. 2023; Cui et al. 2025 [1, 34]
Semaphorin-3A (Sema3a)	Derepressed upon endothelial miR-145 decline	Cardiac neurovascular denervation, electrical instability, and myocardial dysfunction	Suppressed upon miR-145 restoration, preserving cardiac axon density and rhythm	Wagner et al. 2023 [1]
Granzyme K (GzmK)	Elevated in TteK CD8+ T cells and COVID-19 BALF	Age-related tissue remodeling and organ decline independent of immune aging	Downregulated via miR-145 restoration and NF-κB-fibroblast suppression	Kannangara et al. 2026; Jonsson et al. 2022; Allen et al. 2026; Qi et al. 2019 [1]

Table 2: Candidate Host-Directed p53/NRF2 Modulators, Clinical Status, and Safety Trade-Offs

Compound / Agent	Target & Mechanism	Axis Effect (miR-29 / miR-145 / NF-κB)	Clinical / Preclinical Evidence in COVID-19 or Injury	Key Safety & Phase Considerations
Dimethyl Fumarate (DMF) & 4-OI	KEAP1 alkylation; NRF2 activation	Suppresses NF-κB/IFN-γ; induces NRF2–miR-29 antiviral program	Inhibits SARS-CoV-2 replication and inflammation; DMF FDA-approved for MS [1, 9, 23]	Monitor lymphopenia; pulsatile dosing limits chronic NRF2 risk
Sulforaphane	KEAP1 disruption; NRF2/ARE activator	Activates NRF2, upregulates Parkin and miR-29a-3p/miR-145 crosstalk	Mitigates oxidative and mitochondrial stress across preclinical studies [1, 22, 25]	Well-tolerated; oral bioavailability varies by formulation
Nutlin-3a / MDM2 Antagonists	Blocks MDM2–p53 binding; stabilizes p53	Directly transactivates MIR145 and MIR29, repressing c-Myc, TF, GzmK	Preclinical senescence reversal and miR-145 restoration [1, 25]	Avoid high-dose pro-apoptotic regimens in acute ARDS; evaluate HNF4A/NAD+ [15]
Leonurine	Activates p53/miR-29a-3p signaling	Upregulates miR-29a-3p to suppress cardiac fibroblast fibrosis	Attenuates angiotensin II-stimulated cardiac remodeling [1]	Preclinical cardiovascular evidence; requires human PASC trials
Sevoflurane	Volatile anesthetic / postconditioning	Upregulates miR-145 to suppress GZMK and protect myocardium	Protects against murine myocardial I/R injury [1, 39]	Limited to perioperative/ICU settings; mechanistic proof for miR-145/GZMK
Metformin	AMPK activator / c-Myc inhibitor	Suppresses c-Myc, supports SIRT1/SIRT6 and mitochondrial biogenesis	0.7 percentage-point lower clinician-diagnosed Long COVID in RCT [22, 40, 41]	Favorable safety; contraindicated in severe lactic acidosis or acute renal failure

Vitamin D & Sitagliptin	VDR agonist & DPP-4 inhibitor; SIRT6 activation	Enhances SIRT6, suppresses RUNX2/NF-κB/TF/PCSK9, induces miR-101	Low 1,25(OH)2D linked to severe COVID-19; restores VSMC phenotype [1, 19, 22]	Widely available; monitor serum calcium at high calcitriol doses
Bardoxolone Methyl	Potent triterpenoid NRF2 inducer	Nuclear NRF2 translocation; suppresses NF-κB and oxidative stress	Evaluated in renal and inflammatory trials [25]	Monitor fluid retention in patients with severe myocardial dysfunction

Table 3: Bifurcation Dose-Response Sweep Under Persistent Antigenic Reservoir (S_ext = 0.05)

Therapy Input (U_th)	Viral Load (V)	p53/NRF2 (P)	miR-29 (M_29)	miR-145 (M_145)	NF-κB (N)	IFN-γ (I_γ)	TF	Sema3a (S_3)	GzmK (GK)
0.0	4.570	0.142	0.213	0.060	5.810	12.630	12.466	15.250	18.847
0.2	4.216	0.239	0.341	0.116	4.727	9.224	9.964	12.405	15.011
0.4	3.529	0.376	0.607	0.260	3.407	4.888	6.522	8.473	9.669
0.6 (Threshold)	1.456	0.894	1.865	1.440	0.985	0.414	0.525	0.924	0.702
0.8	0.892	1.424	2.660	2.671	0.479	0.166	0.173	0.324	0.213
1.0	0.808	1.754	2.864	3.116	0.380	0.140	0.146	0.271	0.176
1.2	0.767	2.063	2.978	3.419	0.322	0.128	0.135	0.248	0.161
1.5	0.734	2.512	3.079	3.743	0.265	0.118	0.126	0.229	0.150

Table 4: Pan-Viral Conservation of p53/NRF2 Suppression and c-Myc Hijacking

Virus / Family	Primary Viral Hijacking Mechanism	Impact on p53 / NRF2 / c-Myc / miRNAs	Pathological Sequelae Generalizable to Host-Directed Therapy
SARS-CoV-2 (Coronaviridae)	Nsp2/Nsp3, Spike, Orf7b, KEAP1/PVT1/REST	Suppresses p53 and NRF2; elevates c-Myc; depletes miR-29 and miR-145; activates NF-κB	ARDS, myocarditis, thrombosis, neurovascular decline, and PASC tissue aging [1, 19, 26]
Respiratory Syncytial Virus (RSV)	Promotes p53 degradation and NRF2 loss	Disables host antiviral microRNAs and antioxidant defenses	Severe bronchiolitis, airway inflammation, and epithelial remodeling [1]
Influenza A Virus (Orthomyxoviridae)	Replication-induced metabolic stress and cytokine loops	Upregulates c-Myc and suppresses epithelial repair checkpoints	Severe pneumonia, alveolar damage, and post-viral sequelae [1, 26]
Epstein-Barr Virus (Herpesviridae)	LMP1 and EBNA1 transactivate MYC via NF-κB/STAT	Sustained Warburg reprogramming and protective miRNA repression	Lymphomagenesis, epithelial transformation, and chronic immune dysregulation [26]
Hepatitis B & C Viruses	HBx transcriptional co-activation; HCV Core PI3K/Akt stabilization	Hyperactivates c-Myc; recruits EZH2/H3K27me3 to silence miR-101/miR-145	Chronic hepatic fibrosis, steatosis, and hepatocellular carcinoma [26]
HIV-1 & HPV	Tat/Nef immune activation; E6/E7 degradation of p53/Rb	Unopposed c-Myc signaling and p53 checkpoint inactivation	T-cell exhaustion, accelerated multi-organ aging comorbidities, and mucosal remodeling [26]

Figure Legends

Figure 1. Unified Pathologic and Therapeutic Signaling Architecture of p53 and NRF2

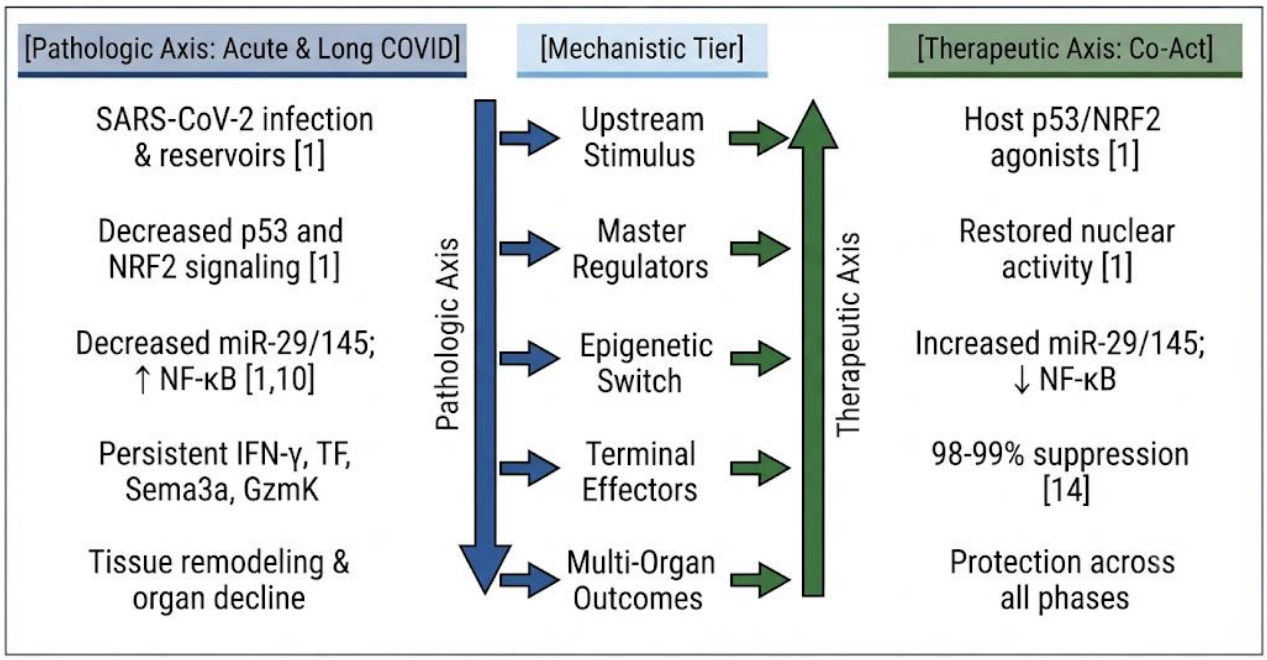


Figure 1. Unified Pathologic and Therapeutic Signaling Architecture of p53 and NRF2 in COVID-19 and Long COVID. Contrastive pathway schematic mapping how SARS-CoV-2 suppresses p53 and NRF2 to collapse miR-29 and miR-145 while hyperactivating NF-κB, unleashing IFN-γ, Tissue Factor (TF), Sema3a, and Granzyme K (GzmK), versus how pharmacological p53/NRF2 co-activation inverts the switch across acute and post-acute phases [1].

Figure 2. Direct Host Antiviral Restriction via the 11 Genomic Binding Sites of the miR-29 Family on SARS-CoV-2

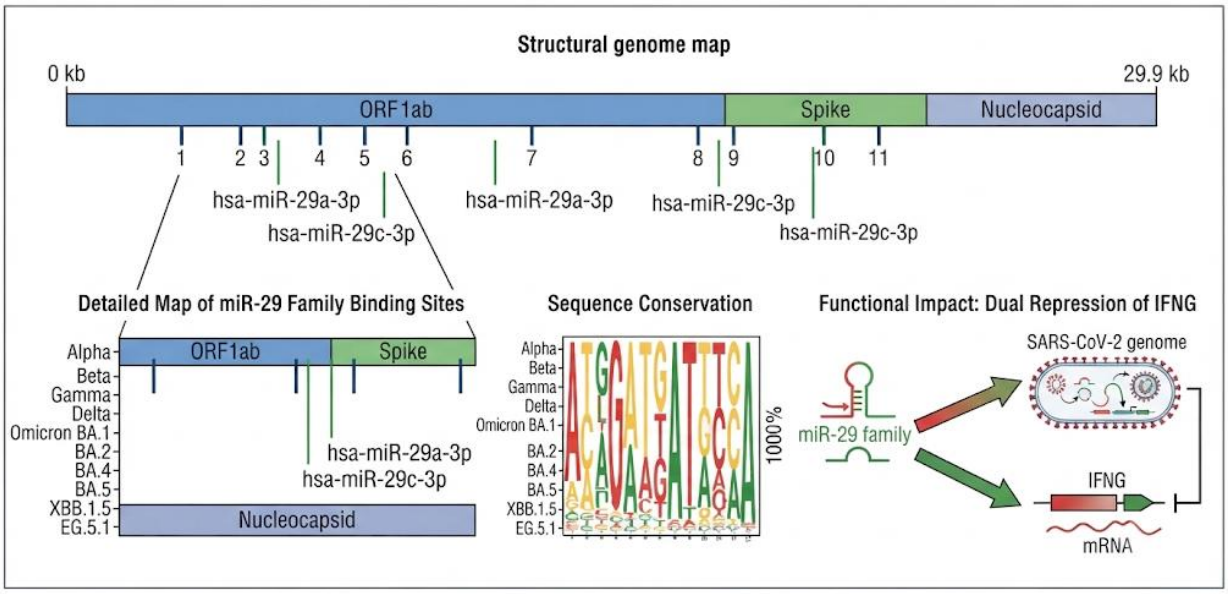


Figure 2. Direct Host Antiviral Restriction via the 11 Genomic Binding Sites of the miR-29 Family on SARS-CoV-2 [1, 10, 29]

Figure 2. Direct Host Antiviral Restriction via the 11 Genomic Binding Sites of the miR-29 Family on SARS-CoV-2. Structural genome map of SARS-CoV-2 (ORF1ab, Spike, and Nucleocapsid regions) displaying the 11 conserved miR-29 family target sites (including 5 sites for hsa-miR-29a-3p and 4 sites for hsa-miR-29c-3p) alongside their 100% sequence conservation across 10 geographic lineages and dual repression of IFNG [1, 10, 29].

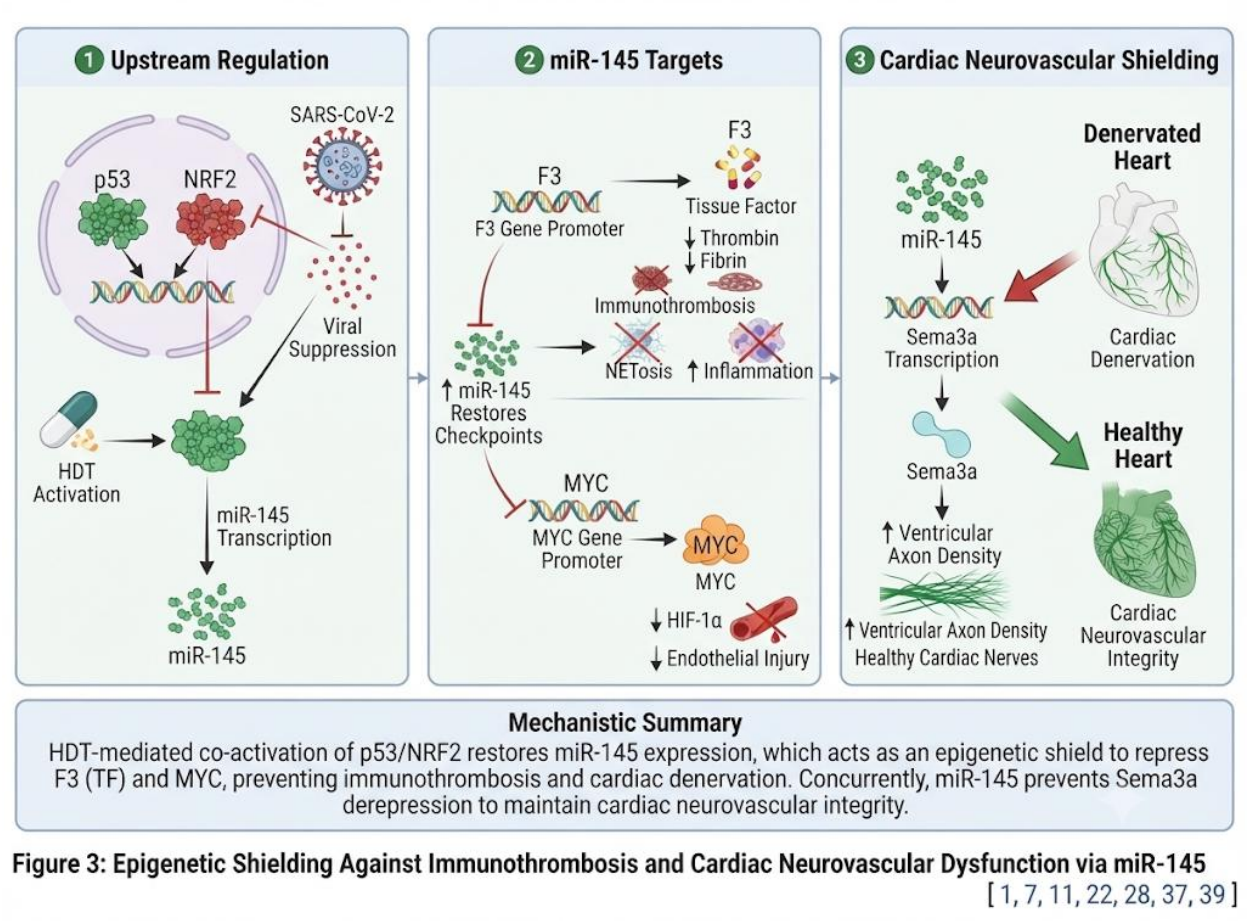


Figure 3: Epigenetic Shielding Against Immunothrombosis and Cardiac Neurovascular Dysfunction via miR-145
[1, 7, 11, 22, 28, 37, 39]

Figure 3. Epigenetic Shielding Against Immunothrombosis and Cardiac Neurovascular Dysfunction via miR-145. Diagram illustrating how p53/NRF2-induced miR-145 targets F3 (Tissue Factor) and MYC while restraining Sema3a derepression, preventing exosomal miR-145-loss-driven thrombosis, cardiac denervation, and electrical instability [1, 7, 11, 28].

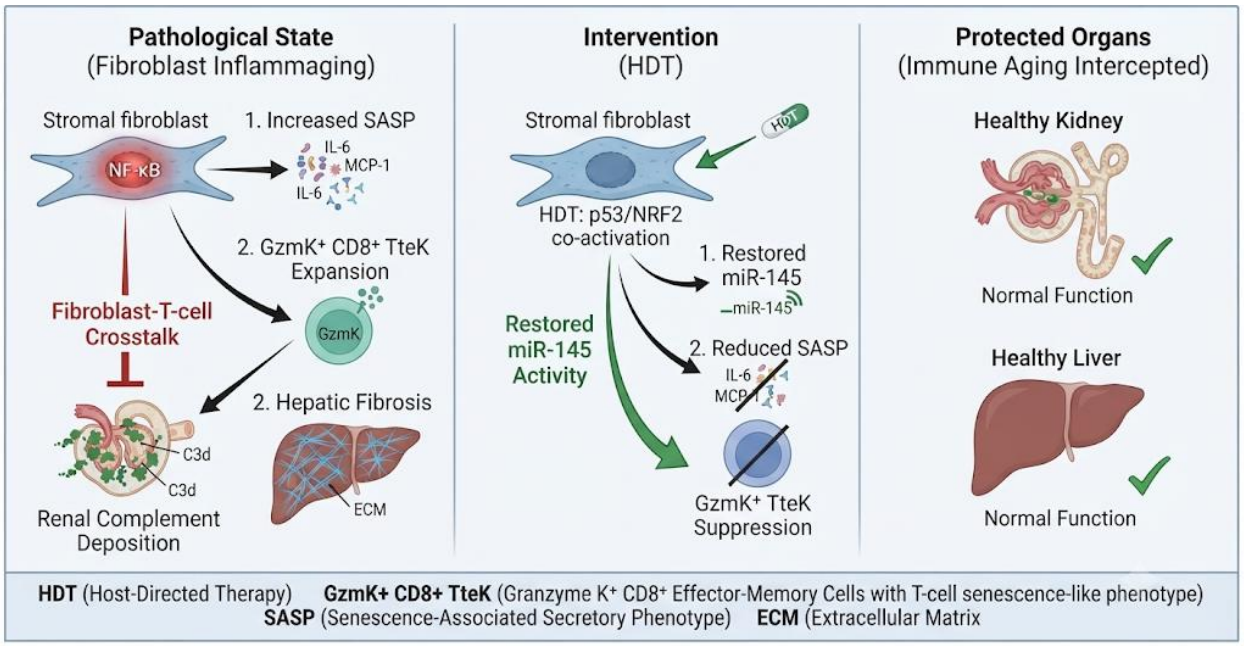


Figure 4. Interception of NF-κB-Activated Fibroblast Inflammaging and Granzyme K-Driven Tissue Remodeling [1, 38, 39]

Figure 4. Interception of NF-κB-Activated Fibroblast Inflammaging and Granzyme K-Driven Tissue Remodeling. Cellular crosstalk model showing NF-κB-activated stromal fibroblasts promoting pro-inflammatory GzmK+ CD8+ TteK cell expansion and immune-independent organ aging (renal complement deposition and hepatic fibrosis), and its suppression via p53/NRF2-driven miR-145 restoration [1, 38, 39].

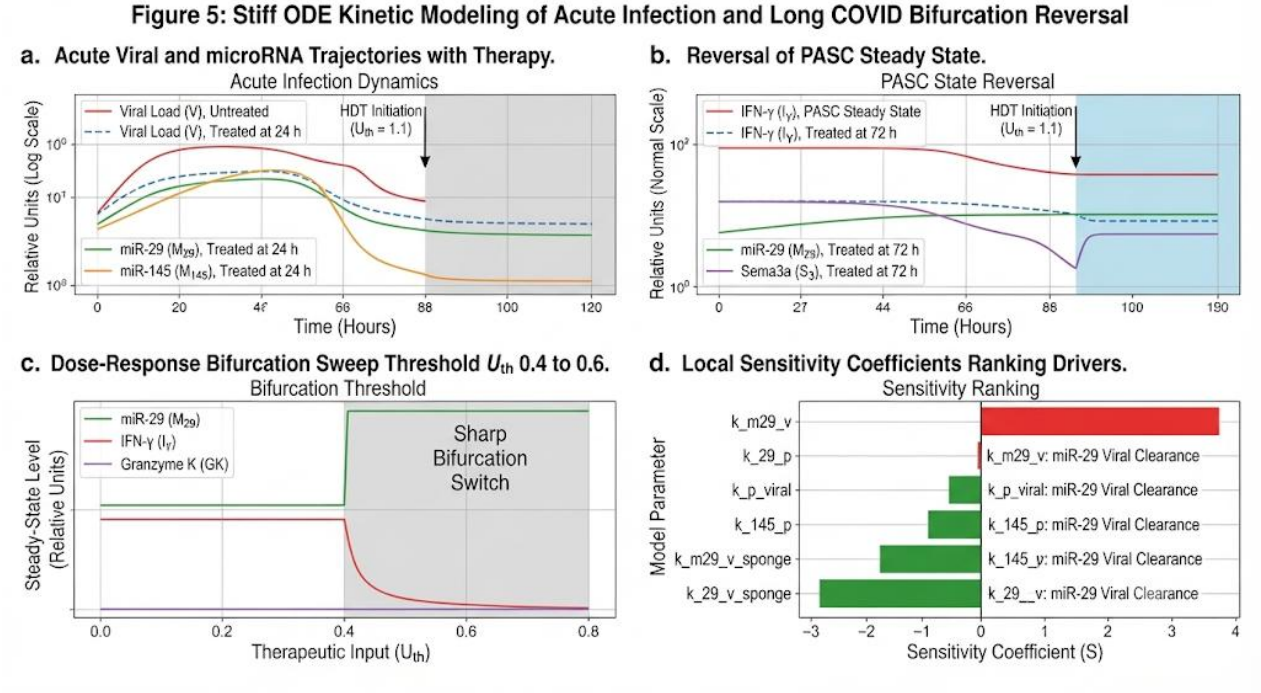


Figure 5. Stiff ODE Kinetic Modeling of Acute Infection and Long COVID Bifurcation Reversal. Numerical solve_ivp/BDF integration curves displaying: (a) acute viral, miR-29/145, and effector trajectories with and without t = 24 h therapy under aggressive replication (r_v = 0.12 h^{-1}); (b) reversal of the locked PASC

steady state (S_ext = 0.05) following therapy at t = 72 h through 504 h; (c) dose-response bifurcation sweep identifying the critical tipping threshold (U_th = 0.4–0.6); and (d) local sensitivity coefficients ranking k_m29_v and k_29_p as dominant system drivers [14].

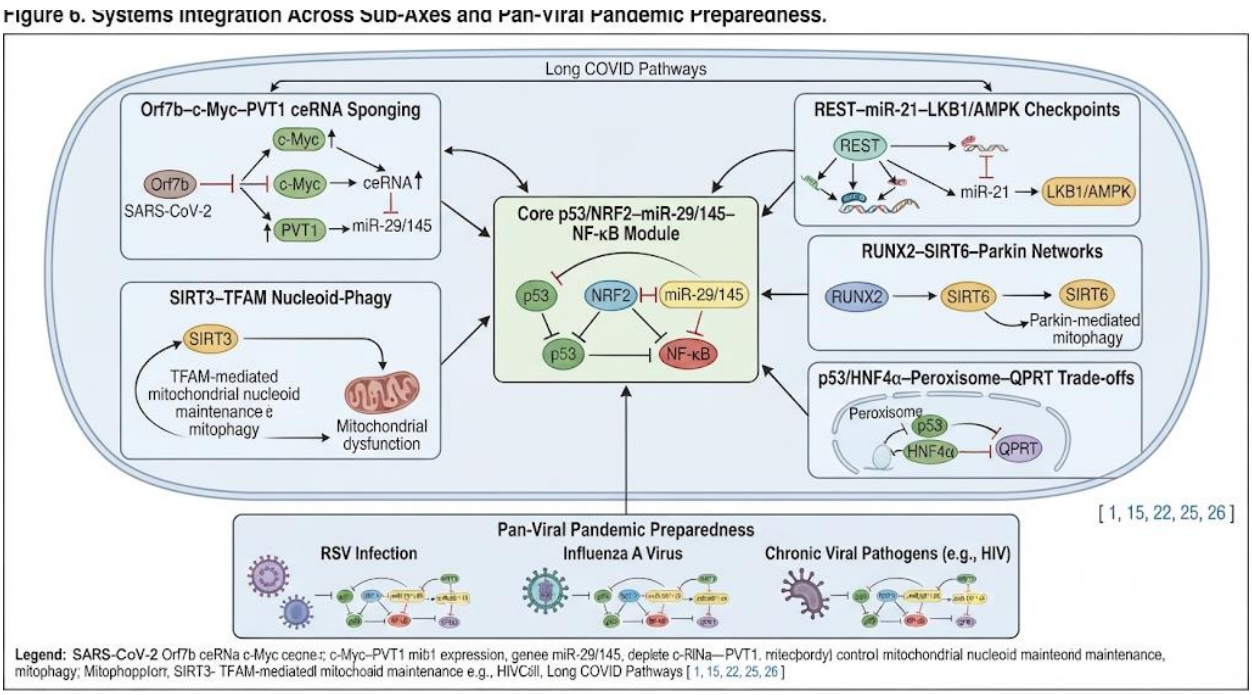
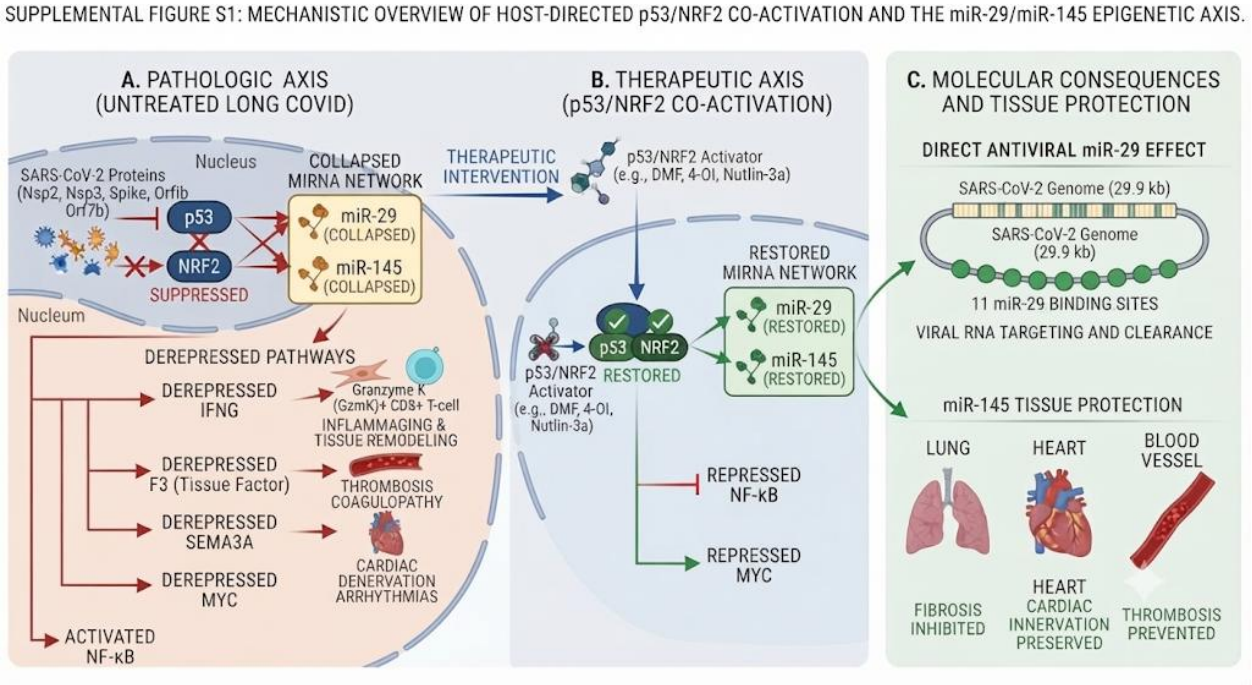


Figure 6. Systems Integration Across Sub-Axes and Pan-Viral Pandemic Preparedness. Multi-scale synthesis connecting the core p53/NRF2–miR-29/145–NF-κB module to secondary Long COVID pathways—including Orf7b–c-Myc–PVT1 ceRNA sponging, SIRT3–TFAM nucleoid-phagy, REST–miR-21–LKB1/AMPK checkpoints, RUNX2–SIRT6–Parkin networks, and p53/HNF4α–peroxisome–QPRT trade-offs—and generalizing to RSV, influenza, and chronic viral pathogens [1, 15, 22, 25, 26].



Supplemental Figure S1: Comprehensive Mechanistic Overview of Host-Directed p53/NRF2 Co-Activation and Epigenetic Axis Restoration Across Acute COVID-19 and Long COVID Pathology.

- (A) Pathologic Axis (Untreated Long COVID / Acute Infection): SARS-CoV-2 viral proteins (such as Nsp2, Nsp3, Spike, and Orf7b) suppress nuclear host stress-response regulators p53 and NRF2. This checkpoint inactivation leads to the transcriptional collapse of protective host microRNA networks, specifically miR-29 and miR-145. The resulting microRNA depletion drives the pathological derepression of downstream effectors: IFNG (promoting GzmK+ CD8+ TteK cell-mediated inflammaging and tissue remodeling), F3 (Tissue Factor) (driving immunothrombosis and coagulopathy), SEMA3A (causing cardiac autonomic denervation and arrhythmias), MYC, and hyperactivated NF-κB.
- (B) Therapeutic Axis (p53/NRF2 Co-Activation): Administration of host-directed activators (such as dimethyl fumarate [DMF], 4-octyl-itaconate [4-OI], and Nutlin-3a) restores nuclear p53 and NRF2 transcriptional activity. Restored p53/NRF2 signaling reactivates the protective miR-29 and miR-145 epigenetic networks while exerting targeted inhibitory control, directly repressing pathological NF-κB and MYC expression.
- (C) Molecular Consequences and Tissue Protection: Restored miR-29 directly engages 11 conserved target sites across the SARS-CoV-2 genome (29.9 kb) to facilitate viral RNA clearance and repress *IFNG*. Simultaneously, restored miR-145 provides broad multi-organ protection—inhibiting pulmonary fibrosis, preserving ventricular myocardial innervation and axon density, and preventing microvascular immunothrombosis across vulnerable tissues.

Back Matter

Author and Institutional Attribution

Dr. L. Boominathan, PhD, Founder and Director-President, Genome-2-BioMedicine Discovery Center (GBMD), Puducherry-4, India. Website: www.genomediscovery.org | Emails: Drboomi@genomediscovery.org, genomdiscovery@gmail.com | Telephone: +91-413-2960879 [1].

Acknowledgments

This independent research was conducted without external institutional grants or commercial funding. Deep appreciation is dedicated to the author's 79-year-old mother, whose daily resilience against chronic respiratory illness (asthma and COPD) provided the moral anchorage and clinical urgency behind this work, and to the Genome-2-BioMedicine Discovery Center (GBMD) for computational infrastructure [1, 22].

Author Contributions

Dr. L. Boominathan, PhD conceived the pathologic and therapeutic axes, curated the multi-study clinical and molecular evidence, formulated the systems-biology architecture and stiff ODE modeling framework, integrated the bioinformatics and priority datasets, and authored the manuscript independently [1, 22, 25].

Competing Interests

The author declares no competing financial or non-financial interests [1, 22, 25].

Funding

This study received no external grants or commercial funding and was supported entirely by the Genome-2-BioMedicine Discovery Center (GBMD), Puducherry, India [22].

Data and Code Availability

All stiff ODE parameter configurations, simulation outputs, and supporting bioinformatic synthesis records generated in this study are archived via the Genome-2-BioMedicine Discovery Center repository (https://genomediscovery.org) and derived from peer-reviewed literature cited below [1, 22, 25].

References

1. Krishna BA, et al. Spontaneous, persistent, T cell-dependent IFN-γ release in patients who progress to Long Covid. Sci Adv. 2024;10(8):eadi9379.

2. Li C, et al. Comparative single-cell analysis reveals IFN-γ as a driver of respiratory sequelae after acute COVID-19. Sci Transl Med. 2024;16(756):eadn0136.

3. Cao X, et al. Inhibition of CXCL10 and IFN-γ ameliorates myocarditis in preclinical models of SARS-CoV-2 mRNA vaccination. Sci Transl Med. 2025;17(828):eadq0143.

4. Kannangara D, et al. Granzyme K is a driver of age-related tissue remodeling and functional decline independently of age-associated immune dysfunction. Immunity. 2026;59(6):1561-1578.

5. Jonsson AH, et al. Granzyme K+ CD8 T cells form a core population in inflamed human tissue. Sci Transl Med. 2022;14(649):eabo0686.

6. Allen NC, et al. NF-κB-activated fibroblasts orchestrate inflammaging and emergence of pro-inflammatory granzyme K+ T cells. Immunity. 2026;59(6):1561-1578.

7. Qi Z, et al. Role of microRNA-145 in protection against myocardial ischemia/reperfusion injury in mice by regulating expression of GZMK. J Cell Physiol. 2019;234(9):16526-16539.

8. Kim IS, et al. Dysregulated thrombospondin 1 and miRNA-29a-3p in severe COVID-19. Sci Rep. 2022;12(1):21227.

9. Gambardella J, et al. Exosomal miR-145 and miR-885 Regulate Thrombosis in COVID-19. J Pharmacol Exp Ther. 2023;384(1):109-115.

10. Ma F, et al. The microRNA miR-29 controls innate and adaptive immune responses to intracellular bacterial infection by targeting interferon-γ. Nat Immunol. 2011;12(9):861-869.

11. Xi T, et al. The p53/miR-29a-3p axis mediates the antifibrotic effect of leonurine on angiotensin II-stimulated rat cardiac fibroblasts. Exp Cell Res. 2023;426(1):113556.

12. Tian R, et al. Restoration of NRF2 attenuates myocardial ischemia reperfusion injury through mediating microRNA-29a-3p/CCNT2 axis. Biofactors. 2021;47(3):414-426.

13. Kurinna S, et al. A novel Nrf2-miR-29-desmocollin-2 axis regulates desmosome function in keratinocytes. Nat Commun. 2014;5:5099.

14. Xiao X, et al. Single-cell RNA sequencing reveals that NRF2 regulates vascular smooth muscle cell phenotypic switching in abdominal aortic aneurysm. FASEB J. 2024;38(13):e23707.

15. Sachdeva M, et al. p53 represses c-Myc through induction of the tumor suppressor miR-145. Proc Natl Acad Sci U S A. 2009;106(9):3207-3212.

16. Olagnier D, et al. SARS-CoV2-mediated suppression of NRF2-signaling reveals potent antiviral and anti-inflammatory activity of 4-octyl-itaconate and dimethyl fumarate. Nat Commun. 2020;11(1):4938.

17. Gómez-Carballa A, et al. Is SARS-CoV-2 an oncogenic virus? J Infect. 2022;85(5):573-607.

18. Zhang S, El-Deiry WS. Transfected SARS-CoV-2 spike DNA for mammalian cell expression inhibits p53 activation of p21(WAF1)... Oncotarget. 2024;15:275-284.

19. Sahu A, et al. MicroRNA-145 Impedes Thrombus Formation via Targeting Tissue Factor in Venous Thrombosis. EBioMedicine. 2017;26:175-186.

20. Wagner JUG, et al. Aging impairs the neurovascular interface in the heart. Science. 2023;381(6660):897-906.

21. Jafarinejad-Farsangi S, et al. High affinity of host human microRNAs to SARS-CoV-2 genome: An in silico analysis. Noncoding RNA Res. 2020;5(4):222-231.

22. Al-Aly Z, et al. Long COVID science, research and policy. Nat Med. 2024;30:2148–2164.

23. Msemburi W, et al. The WHO estimates of excess mortality associated with the COVID-19 pandemic. Nature. 2022;613:130–137.

24. Thomas D, et al. CCL2-mediated endothelial injury drives cardiac dysfunction in long COVID. Nat Cardiovasc Res. 2024;3(10):1249–1265.

25. Cui J, et al. Inhibiting NINJ1-dependent plasma membrane rupture protects against inflammasome-induced blood coagulation and inflammation. eLife. 2025;12:RP91329.

26. Wei X, et al. Macrophage peroxisomes guide alveolar regeneration and limit SARS-CoV-2 tissue sequelae. Science. 2025;387(6738):eadq2509.

27. Maeda Y, et al. Tumour suppressor p53 down-regulates the expression of the human hepatocyte nuclear factor 4alpha (HNF4alpha) gene. Biochem J. 2006;400(2):303–313.

28. Dalle Carbonare L, et al. Extracellular vesicles from long COVID patients promote RUNX2-mediated cellular stress via dysregulated miR-204 and p53 pathway activation. Cell Commun Signal. 2025;23(1):508.

Priority Discovery Logs and Preprint Archive (2020–2026)

1. Boominathan L. 931+ discovery posts on COVID-19 and other viruses (2020–2026): https://x.com/DrLBoominathan/status/1665034484524122114.

2. Boominathan L. Priority post on p53/NRF2-based therapy for treating COVID-19 and other infectious diseases (18 Sept 2023; 134.5K impressions): https://x.com/DrLBoominathan/status/1716267826829549863.

3. Boominathan L. Day-to-day viral discovery timeline (2020–2026): https://x.com/DrLBoominathan.

4. Boominathan L. Tumor Suppressors Are Longevity Genes: A Conceptual Shift in Cancer Biology. ResearchSquare. Sep 15, 2026.

5. Boominathan L. A Universal Host-Directed Antiviral Platform: Unifying the p53/p21/NRF2 Axis... ResearchSquare. Sep 20, 2026.

6. Boominathan L. COVID-19 Accelerates Cardiac Ageing via p53–miR-145 Axis Collapse and PVT1/IL-11/IL-33-Mediated Lymphatic Degeneration. ResearchSquare. Oct 06, 2026.

7. Boominathan L. Molecular Mechanism of Psilocybin-Induced Longevity: The c-Fos–SIRT6 Epigenetic Axis. ResearchSquare. Oct 08, 2026.

8. Boominathan L. The Unified Systems Theory of PASC: Resolving the Ferroptosis-Replication Loop and the Bioenergetic Lock. ResearchSquare. Oct 12, 2026.

9. Boominathan L. The REST/STAT3-miR-21 Axis Drives Premature Biological Aging and Mortality in Severe COVID-19... ResearchSquare. Oct 13, 2026.

10. Boominathan L. Targeting the p53–TFAM Axis to Overcome Exercise Intolerance in Long COVID. ResearchSquare. Oct 19, 2026.

11. Boominathan L. Restoring the p53--Nrf2--SIRT3--TFAM Axis via Therapeutic Epigenetic Shielding... ResearchSquare. Oct 22, 2026.

12. Boominathan L. Auditory Epigenetic Transduction: Acoustic Perception Drives the c-Fos–SIRT6–SIRT3–Dicer Axis... ResearchSquare. Oct 25, 2026.

13. Boominathan L. Reclaiming the Host: Why p53/NRF2-Directed Therapies Should Enter the Global Antiviral Policy Agenda. Preprints.org. Oct 27, 2026.

14. Boominathan L. Systems Integration of the SARS-CoV-2 ORF7b–c-Myc–PVT1–miR-145/214–HIF-2α–TFRC–CCL2 Axis in Long COVID... Preprints.org. Nov 09, 2026.

Supplementary Files

This is a list of supplementary files associated with this preprint. Click to download.

- Suppfig1.png